Available online at www.sciencedirect.com
ScienceDirect
Journal of the European Ceramic Society 31 (2011) 1889–1895
www.elsevier.com/locate/jeurceramsoc

Ceramic matrix composites in the alumina/5–30 vol.% YAG system

R. Lach, K. Haberko *, M.M. Bućko, M. Szumera, G. Grabowski

AGH University of Science and Technology, Al. Mickiewicza 30, 30-059 Krakow, Poland

Received 29 July 2010; received in revised form 22 March 2011; accepted 3 April 2011
Available online 27 April 2011

Abstract

The preparation technique of the particulate composite materials in the alumina/YAG system was elaborated. Within alumina particles suspension yttria precursor was precipitated with ammonium carbonate. Drying and calcination at 600 °C resulted in the mixture of alumina and yttria particles, the latter being much finer than alumina particles. This mixture was additionally homogenized by short attrition milling in an aqueous suspension. Sintering of such powders results in the materials composed of YAG inclusions of sizes smaller than shown by alumina grains and evenly distributed within the matrix. YAG particles result from the reaction of Y_2O_3 with Al_2O_3 during heat treatment. YAG inclusions limit effectively grain growth of the alumina matrix. Hardness, fracture toughness, strength, Young modulus and wear susceptibility of composites and pure alumina were measured. Composites show higher hardness and in some cases higher fracture toughness and wear resistance than pure alumina polycrystals.

Keywords: Ceramic matrix composites; Alumina; YAG

1. Introduction

Alumina is one of the most frequently used structural material. Its generally good mechanical properties, especially fracture toughness, can be improved by the second phase inclusions. Alumina/zirconia composite is a well known example.[1] YAG ($Y_3Al_5O_{12}$) seems to be an alternative inclusion phase. This is one of the three phases in the Al_2O_3–Y_2O_3 system. $YAlO_3$ and $Y_4Al_2O_9$ are the other ones. Among these phases YAG is characterized by the highest aluminum content. That is why it is stable in contact with alumina and should be the final inclusion phase in the powder mixture of yttria with the surplus amount of alumina.

Some articles on the alumina/YAG composites describe materials prepared by the directional eutectic crystallization.[2–9] The application of very high temperatures necessary to melt these compositions is a characteristic feature of this technique. This is the reason of several researchers' efforts to prepare composites in this system by the powder/sintering technology. Co-precipitation was one of the applied powder preparation techniques. Using aluminum and yttrium nitrates[10,11] or chlorides[12] treated with ammonia, gels were prepared. Their calcination resulted in powders of YAG content of 25, 5 and 50 vol.%, respectively. Such powders were densified either by hot pressing[10,11] or pressure-less sintering.[12] Sol–gel techniques should also be mentioned as a method of YAG-alumina composite fibers preparation.[13,14] In these cases relative alkoxides or chlorides were applied.

Another group of investigations on Al_2O_3/YAG composites is based on mixing alumina with yttria[15] or yttria precursors (yttrium nitrate,[16] yttrium chloride,[17,18] yttrium alkoxides[19,20] and YAG powder).[21] Subsequent heat treatment of the powders resulted in composites of different YAG content. Materials in the Al_2O_3–YAG–ZrO_2 triple system should also be mentioned.[22]

The aim of the present study was to elaborate a new, not applied till now, technique of alumina/YAG composites preparation covering broad YAG contents from 5 to 30 vol.%. The technique is based on precipitation of yttria precursor within alumina grain suspension. Reactions occurring at elevated temperatures within yttria precursor and between yttria and alumina are shown. It allowed us to optimize the starting powders preparation conditions as well as sintering conditions of the system. The effect of YAG inclusion concentrations on grain sizes of alumina and YAG particles is presented. Selected mechanical properties of the materials are shown. An effort is made to identify mechanism of fracture toughness increase caused by the YAG inclusions present in the dense composites. In order to

* Corresponding author. Tel.: +48 12 617 25 07.
E-mail addresses: radek.lach@poczta.fm (R. Lach), haberko@agh.edu.pl (K. Haberko).

0955-2219/$ – see front matter © 2011 Elsevier Ltd. All rights reserved.
doi:10.1016/j.jeurceramsoc.2011.04.003

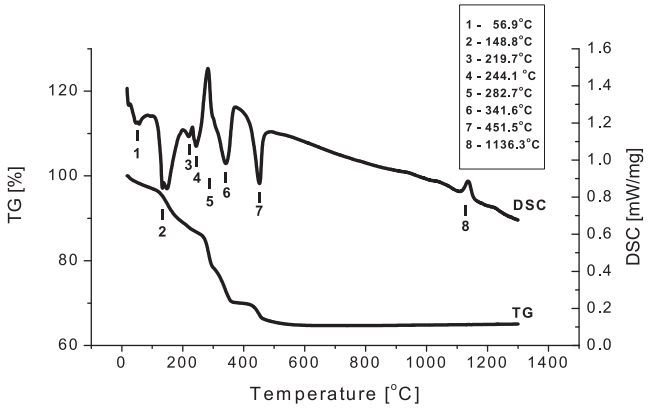

Fig. 1. DSC/TG curves of the yttria precursor and alumina mixture. Yttria content corresponds to YAG 20 vol.% after the reaction of the system. Rate of temperature increase 10 °C/min.

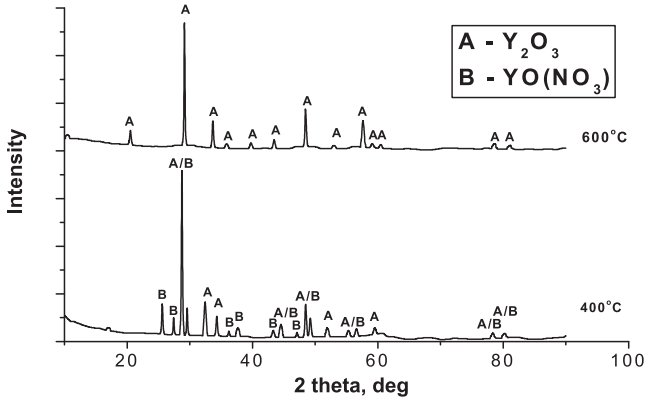

Fig. 3. X-ray diffraction pattern of yttria precursor heated up to indicated temperatures.

approach to the possible practical applications of these composites their wear resistance are measured. For the sake of comparison also pure alumna and standard 3YTZP materials were used.

2. Experimental

Alumina (TM DAR TaiMai Chemicals, Japan) and yttria of purity 99.99% (Aldrich) were used. Yttria was dissolved in nitric acid (analytical quality). The resulting $Y(NO_3)_3$ solution was introduced into the alumina aqueous suspension of 50 vol.% concentration in quantities corresponding to YAG content 5, 10, 20 and 30 vol.% after the reaction within the system. The vigorously stirred suspension was treated with the ammonium carbonate solution until the suspension reached pH 8.5. Under such conditions the quantitative yttria precursor precipitation occurs, as determined by the ICP analysis of the filtrate. The suspension was dried at 100 °C and calcined at 600 °C for 60 min. Before drying no washing was applied. The resulting powder, composed of Al_2O_3 and Y_2O_3, was attrition ground for 30 min using zirconia 2 mm balls (TOSOH). Weight ratio of the powder to grinding media corresponded to 1: 20. Grinding was performed in water (70 cm^3/100 g of powder) at pH 8, received with $(NH_4)_2CO_3$ additive. According to our previous studies[23,24] under such conditions no contamination of the system with zirconia occurs and its good homogenization can be achieved. The powders were dried for 12 h at 100 °C and separated from the grinding media on a sieve. Cylindrical samples of 25 mm diameter and 2.5–3 mm thickness were uniaxially compacted under 50 MPa and isostatically repressed under 300 MPa. Then the compacts were sintered in air atmosphere at 1400, 1500 and 1600 °C with the rate of temperature increase 5 °C/min., 2 h soaking time and cooling with the furnace.

Alumina and alumina/yttria powders were characterized by the specific surface area measurements using nitrogen adsorption (Quantachrome, Nova 1200). DSC/TG measurements (Netzsch STA 449 F3 Jupiter) were used to follow the phenomena occurring during heat treatment of the powder samples. The identification of gases emitted by the samples at elevated temperatures (Mass Spectrometer QMD 300 Thermostar, Balzers) was helpful in understanding these phenomena. Green samples were characterized by pore size distribution measurements (Quantachrome, PoreMaster). In order to follow shrinkage, dilatometric measurements were performed using Netzsch equipment (DIL 402C). Hydrostatic weighing allowed us to determine apparent density of the sintered samples.

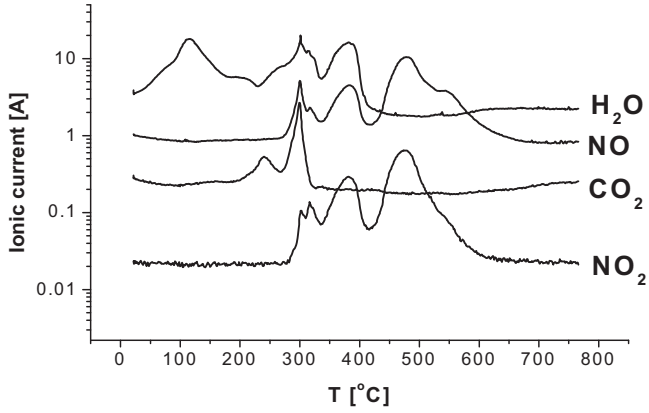

Fig. 2. Gasses emitted by the yttria precursor precipitated under the same conditions as applied on the alumina/yttria precursor preparation. Rate of temperature increase 10 °C/min.

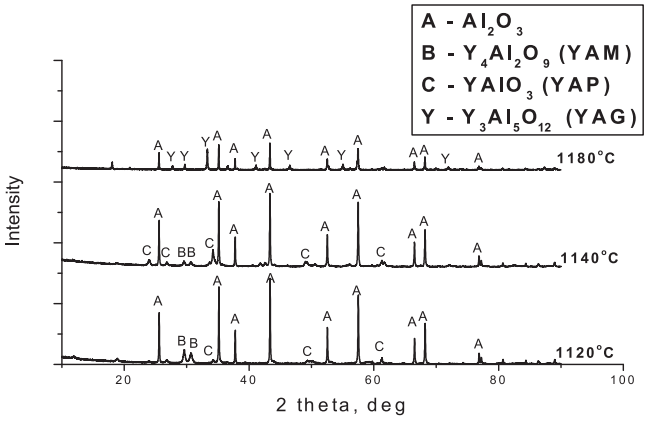

Fig. 4. X-ray diffraction pattern of alumina/yttria mixture calcined in DSC/TG equipment at indicated temperatures. Yttria content corresponds to YAG 20 vol.% after the reaction of the system.

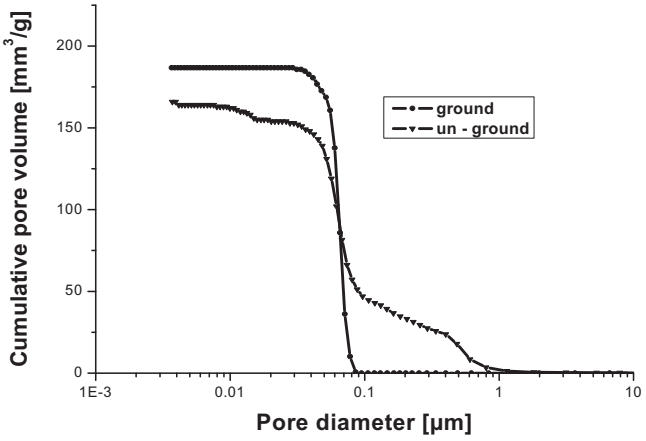

Fig. 5. Cumulative curves of the pore size distribution in compacts of attrition ground and un-ground composite powder of yttria content corresponding to 20 vol.% YAG fraction after completion of the reaction. Isostatic compaction pressure 300 MPa.

Fracture toughness and hardness were measured by the Vickers indentation using Future Tech (Japan) equipment. In the former case load of 0.5–1 kgf and in the latter one 3–10 kgf were applied. No cracks occurred when lower load was applied. Critical stress intensity factor (K_{Ic}) was calculated using Niihara formulae[25,26] for the median crack or Palmqvist type fracture depending on the *c*/*a* ratio, where c is radius of the surface crack and a is the half-diagonal of the Vickers indent. For $c/a > 2.5$ median crack formula – and below this value – formula corresponding to the Palmqvist crack model were applied.[26] In the letter case additionally *l*/*a* ratio was tested, where *l* is Palmqvist crack length. The observed *l*/*a* ratio values were within the range of 1–2.5 foreseen for this type of cracks.[26] The Palmqvist cracks were observed in the composite of 20 vol.% YAG (AY20) content sintered at 1500 °C and 1600 °C. Another strong premise justifying application the Palmqvist crack model in cases of *c*/*a* values even slightly below 2.5 and essentially below the upper *l*/*a* ratio (see Table 5) comes from the observed by us separation of the cracks from the indent in the polished sample surface. This is indicated in the literature[27] as a criterion of this type of cracks.

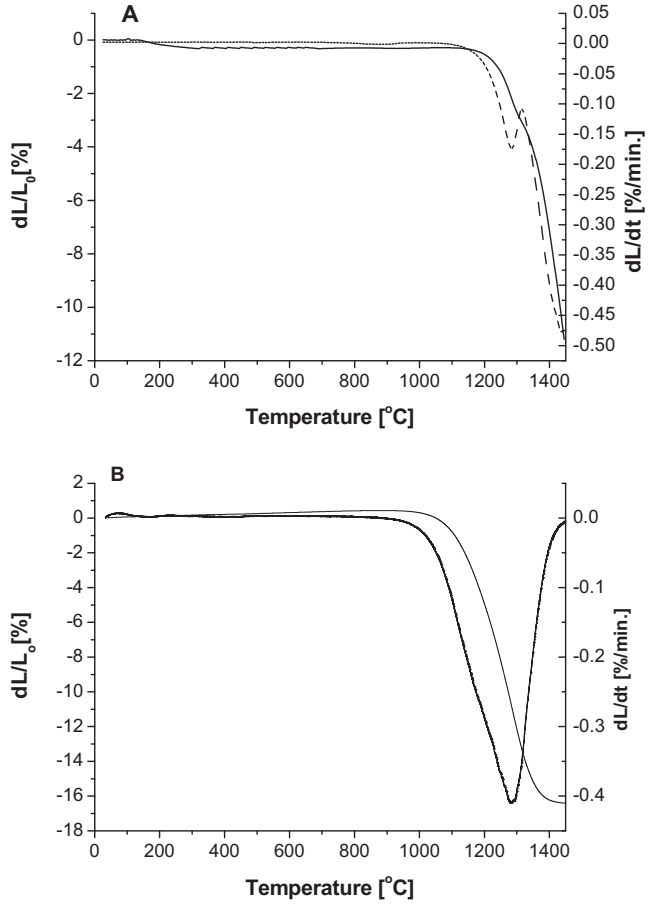

Fig. 6. Dilatometric and derivative (dashed lines) curves of the composite (A) and pure alumina (B) powders. Composite powder (A) contains Y_2O_3 corresponding to 20 vol.% YAG after atria/alumina reaction. Isostatic compaction pressure 300 MPa. Rate of temperature increase 10 °C/min.

Table 1
Specific surface area (S_w) of the Y_2O_3/Al_2O_3 mixtures, alumina and sizes (D_{BET}) of yttria and alumina particles.

Composition	Al_2O_3	AY5	AY10	AY20	AY30
S_w, m^2/g	12.4	13.72	14.97	17.50	19.44
D_{BET}, nm	121.3	22.5	22.8	22.9	24.0

S_w shows pure alumina and alumina/yttria mixture surface area corresponding to YAG volume fraction after the reaction and D_{BET} alumina and yttria particle sizes. Symbols AY5–AY30 correspond to the compositions of indicated YAG vol.% after alumina/yttria reaction.

Table 2
Relative density [% theo] of the sintered samples.

Composition	1400 °C	1500 °C	1600 °C
Al_2O_3	99.53 ± 0.06	99.38 ± 0.04	99.05 ± 0.11
AY5	93.28 ± 0.03	99.23 ± 0.02	99.28 ± 0.01
AY10	90.94 ± 0.03	98.33 ± 0.05	99.01 ± 0.02
AY20	81.91 ± 0.01	97.63 ± 0.05	99.53 ± 0.06
AY30	78.95 ± 0.07	95.55 ± 0.06	99.02 ± 0.10

Relative density was calculated assuming alumina density 3.99 cm^3/g and YAG density 4.55 cm^3/g.
± confidence interval at 0.95 confidence level.

Phase compositions of the sintered samples were determined by the X-ray diffraction (CuK_α radiation, equipment X'Pert Pro, Panalytical). Elastic properties were determined by the ultrasonic method.[28] The biaxial fracture test piston-on-three ball test according to ISO 6872:2008(E) allowed us to measure mechanical strengths of the materials. Load was applied

Table 3
Grain sizes [μm] of alumina and YAG particles.

Material	1400 °C		1500 °C		1600 °C	
	Al_2O_3	YAG	Al_2O_3	YAG	Al_2O_3	YAG
Al_2O_3	1.25	–	2.07	-	4.87	-
AY5	–	–	0.74	0.32	1.19	0.55
AY10	–	–	0.62	0.28	1.13	0.48
AY20	–	–	0.45	0.29	0.88	047
AY30	–	–	0.48	0.33	0.95	0.54

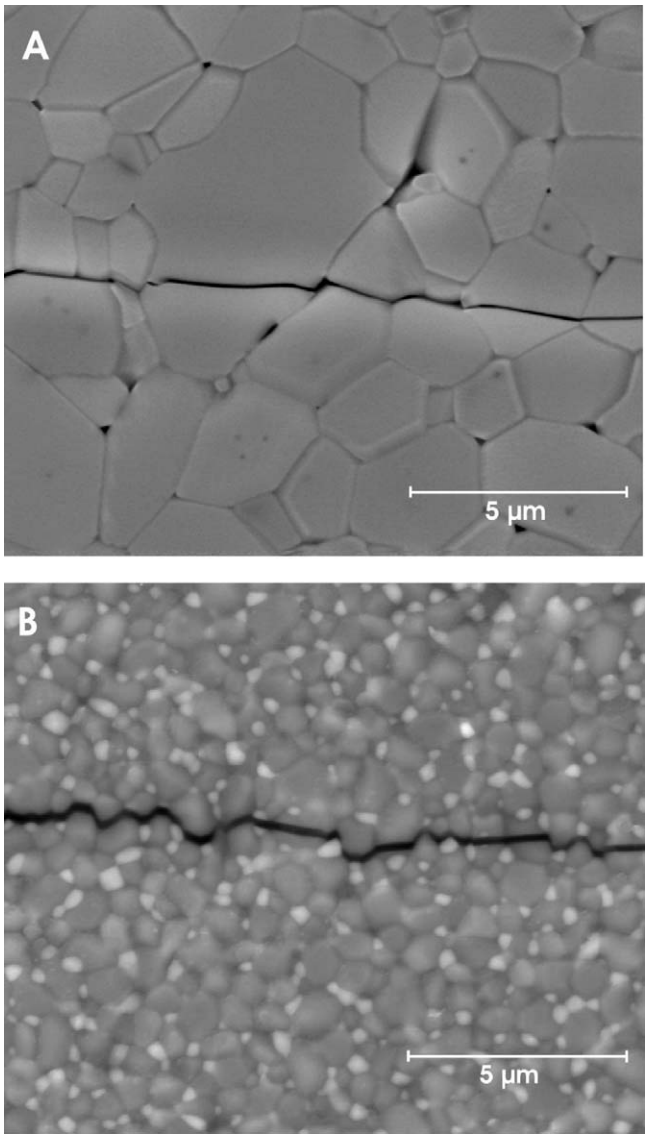

Fig. 7. SEM micrographs of materials sintered at 1500 °C, (A) alumina and (B) composite of 10 vol.% YAG, crack path shown.

using the Zwick/Roell Z150 machine. The samples used to determine strengths, fracture toughness and hardness were polished with the proper diamond suspensions and, finally, with colloidal silica. Thermal etching at 1400 °C for 6 h revealed grain and interface boundaries. Macrostructures were observed with the scanning electron microscope (FEI Nova Nano SEM 200). Mean intersect of alumina and YAG grains was used as a measure of their sizes.

Wear susceptibility was determined using ASTM G 6585 Dry Send Test. Steel weal covered with rubber was pressed against the tested surface with the load of 44N. Between the sample and rotating weal of diameter 49 mm and thickness 8.3 mm, the abrasive SiC powder of 0.5 mm grain sizes was introduced. Change of the sample weight after 2000 revolutions of the weal recalculated to volume of the worn out sample volume was a measure of the wear susceptibility.

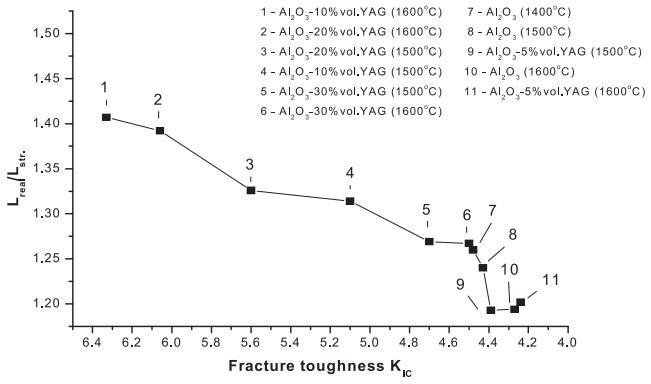

Fig. 8. $L_{real}/L_{str.}$ vs. K_{Ic}.

3. Results and discussion

Measurements were performed using powder mixture which, after alumina and yttria precursor calcination at sufficiently high temperature, should result in 20 vol.% YAG concentration. Fig. 1 shows DSC/TG curves of such a powder mixture. Heat effects corresponding to the points 1–6 indicated in the graph result probably from the mixture composition: Presence of yttrium oxycarbonate,[29] ammonium nitrate and hydrous yttria precursor can be postulated. Their decomposition at elevated temperature results in water vapour, nitrogen oxides and carbon dioxide emission. This is really the case as it is corroborated by the data in Fig. 2. In order to identify the reason of the effect marked by the point 7 in Fig. 1, pure yttria precursor was heated using our DSC/TG equipment to the temperatures below and above minimum of this endothermic effect and quickly cooled down. In Fig. 3 X-ray diffraction patterns of the materials resulting from such a treatment are shown. It is obvious that the endothermic effect with minimum at 451 °C results from the decomposition of yttrium oxy-nitrate, $YO(NO_3)$. This is accompanied by NO and NO_2 emission (see Fig. 2) and change of the sample weight (see Fig. 1). The sample calcined at 600 °C shows yttria presence only.

In Fig. 1 we observe the exothermic effect with maximum at 1136 °C (point 8). Using our DSC/TG equipment the samples of the material were heated up to temperatures covering the range of this effect. After reaching the predetermined temperature the samples were quickly cooled down. Fig. 4 demonstrates X-ray diffraction patterns of these samples. In the samples heated up to 1120 °C and 1140 °C YAM and YAP could be identified. Temperature 1180 °C is sufficient to get full reaction of Al_2O_3 and Y_2O_3 resulting in YAG synthesis. So it is evident that the reaction of Y_2O_3 with Al_2O_3 is responsible for the mentioned exothermic effect.

All alumina/yttria precursor powders were calcined at 600 °C. Due to hard agglomerates formed under such calcination conditions, the compacts of such powders show bi-modal pore size distribution (Fig. 5). Larger pores correspond to inter-agglomerate space and smaller ones to intra–agglomerate pore volume.[30] Such powder characteristics are detrimental from the point of view of sintering ability.[31,32] A short duration of attrition milling, using zirconia grinding media, removes agglomerates

Table 4
Hardness (HV), Young modulus (E), strength (σ) and volume of the material removed by the "dry send test" (V) of alumina and composites.

Material sintered at temperature	HV [GPa]	E [GPa]	σ [MPa]	V [mm^3]
Al_2O_3, 1400 °C	16.44 ± 0.58	369·0 ± 8.4	425 ± 50	16·6
Al_2O_3, 1500 °C	16.55 ± 0.32	365·0 ± 6.36	476 ± 61	48·7
Al_2O_3, 1600 °C	15.47 ± 0.40	365·2 ± 5.4	422 ± 79	58·7
AY5, 1500 °C	19.43 ± 0.57	335·8 ± 15.6	232 ± 18	10·9
AY5, 1600 °C	18.65 ± 0.52	341·8 ± 6.7	203 ± 19	27·8
AY10, 1500 °C	18.89 ± 0.92	349·2 ± 8.5	376 ± 74	5·7
AY10, 1600 °C	19.51 ± 0.51	341·7 ± 8.1	579 ± 31	20·8
AY20, 1500 °C	19.46 ± 0.59	341·4 ± 4.6	325 ± 50	5·9
AY20, 1600 °C	19.20 ± 0.63	347·9 ± 9.0	355 ± 42	13·1
AY30, 1500 °C	18.71 ± 0.74	308·2 ± 7.2	318 ± 99	7·6
AY30, 1600 °C	18.42 ± 0.10	348·3 ± 3.54	305 ± 113	12·5

± confidence interval at 0.95 confidence level.

as it is demonstrated by the mono-modal pore size distribution in this powder compact and does not lead to the system contamination with the uncontrolled zirconia admixture.

In Table 1 specific surface area values of the attrition ground powders are shown. Basing on these measurements and the known yttria/alumina proportions alumina and yttria particle sizes could be assessed using the $D_{BET} = 6/d{\cdot}S_w$ formula, assuming density (d) 3.99 g/cm^3 and 5.01 g/cm^3 of alumina and yttria, respectively. These data indicate that the yttria particles are much smaller than the alumina ones. It should result in smaller YAG particles than the size of the alumina matrix grains and it is shown below that this was the case (see further text).

Fig. 6 demonstrates results of the dilatometric measurements of the composite powder compact (Fig. 6A) and compact of pure alumina (Fig. 6B). Temporary slowing down of the system densification occurs in the case of the composite powder. Onset of this phenomenon agrees well with the data of Figs. 1 and 4. So, it seems reasonable to relate this effect to the solid state reaction of Al_2O_3 and Y_2O_3. It is well known that solid state reactions slow down sintering process.[33,34] Another reason of this behaviour, operating in the same direction, can be attributed to the change of the system specific volume due to the phase composition transformation from the $Al_2O_3 + Y_2O_3$ to Al_2O_3 + YAG mixture. Calculations for the composition corresponding to 20 vol.% YAG show that this transformation leads the system volume increase by 1.23%, i.e. 0.41% linear expansion. As it should be expected, no temporary slow down of densification occurs in the single phase alumina compact (Fig. 6B).

In Table 2 results of the materials densification are shown. YAG inclusions limit densification of the composites, especially at lower sintering temperatures. All composite samples sintered at 1400 °C show open porosity. The detrimental effect of inert inclusions on densification was also observed in other systems.[35]

Examples of SEM micrographs of the sintered samples are shown in Fig. 7. Crack path is also indicated (see discussion in the further text). Using such micrographs mean values of chords within each observed phase were applied as a relative measure of alumina and YAG grain sizes. The results shown in Table 3 and in Fig. 7 indicate that YAG inclusions effectively slow down alumina grain growth, presumably due to the Zener effect. YAG grains are smaller than the alumina ones. Probably difference in their sizes results from the essentially smaller yttria particles compared to alumina grains in the starting powder (see Table 1).

In Table 4 hardness, Young modules strength and volume of the material removed by the dry send test are shown. Hardness of all well densified composite materials is essentially higher than that of pure alumina polycrystals. Young modulus of the studied composites is lower than observed in pure alumina and drops down with the YAG concentration. This is probably due to the lower modulus of YAG compared to that of Al_2O_3.

Table 5
Fracture toughness (K_{Ic}) of alumina and composites.

Material sintered at temperature	K_{IC} [MPa m$^{1/2}$]	c/a	Nature of cracks
Al_2O_3, 1400 °C	4.48 ± 0.35	3.38	Median
Al_2O_3, 1500 °C	4.43 ± 0.17	2.76	Median
Al_2O_3, 1600 °C	4.27 ± 0.59	2.83	Median
AY5, 1500 °C	4.39 ± 0.52	2.88	Median
AY5, 1600 °C	4.24 ± 0.24	2.94	Median
AY10, 1500 °C	5.10 ± 0.40	3.18	Median
AY10, 1600 °C	6.33 ± 0.70	2.82	Median
AY20, 1500 °C	5.60 ± 0.27	2.45 (l/a = 1.84)	Palmqvist
AY20, 1600 °C	6.06 ± 0.50	2.35 (l/a = 1.45)	Palmqvist
AY30, 1500 °C	4.70 ± 0.59	3.24	Median
AY30, 1600 °C	4.50 ± 0.32	3.49	Median

An essential increase of fracture toughness (Table 5) is observed in the material of 10 and 20 vol.% YAG (AY10, AY20) content compared to the pure alumina polycrystals. Some light on this problem is thrown by the crack path observations (Fig. 7). Cracks were provoked by the Vickers pyramid indentation. In pure alumina polycrystal mainly transgranular cracks occur. This kind of crack path is limited in composites; they are winding. This suggests crack deflection due to the crack interaction with the second phase (YAG) inclusions, a well recognized toughening mechanism.[36,37] In order to verify this observation in a more quantitative way a crack length along its winding way was measured, using SEM micrographs like those in Fig. 7, and related to the straight line length (L_{real}/L_{str}). Then these figures were plotted vs. K_{Ic} values (Fig. 8). The presented data indicate that K_{Ic} is the higher the higher is the L_{real}/L_{str} ratio, clearly pointing out crack deflection as a source of increased AY10 and AY20 composites fracture toughness.

The highest strength and toughness shows material of 10 vol.% YAG content (AY10) sintered at 1600 °C. It is interesting to notice that the alumina matrix size in this case is comparable to that of pure alumina sintered at 1400 °C (see Table 3). This result emphasizes role of inclusions in strengthening and toughening of the material.

Good wear resistance is one of the key properties of ceramics. The complexity of wear means that few reliable general predictions regarding the wear of composites can be made. Results presented in Table 4 show that volume of the material worn out in the "dry send test" increases with sintering temperature. It suggests that this property is dependant on the grain sizes of alumina matrix. Since YAG inclusions reduce Al_2O_3 grain sizes, composites show lower wear susceptibility, i.e. higher wear resistance than pure alumina polycrystal. Best properties show AY10 and AY20 composites sintered at 1500 °C. One of the well known wear resistant oxide materials are tetragonal zirconia polycrystals (TZP). Using commercial 3YTZP powder dense (6.01 g/cm^3) material was prepared and subjected to the wear test under the same conditions as applied case of AY materials. It is interesting to notice that volume of the material removed under these conditions is 11.97 mm^3 what is essentially higher than observed in AY10, AY20 and AY30 sintered at 1500 °C (see Table 4).

4. Conclusions

The elaborated technique of alumina and yttria composite powder preparation results in nanometric Y_2O_3 particles distributed within sub-micrometer Al_2O_3 grains. At elevated temperature reaction between the mixture constituents leads to the YAG particles synthesis. In the intermediate stage YAM and YAP phases appear. Compacts of such powders sintered at sufficiently high temperature result in dense composite materials of YAG concentration 5–30 vol.%. Microscopic observations show that YAG inclusion sizes are smaller than alumina grains. Hardness of these materials is higher than observed in case of pure alumina. The highest fracture toughness is observed in the composites of 10 and 20 vol.% YAG content sintered at 1500 °C and 1600 °C. This is most probably due to the crack deflection mechanism operating in these cases. The highest fracture toughness and strength values occur in the material AY10 sintered at 1600 °C.

Wear resistance seems to be dependant on the alumina matrix grain sizes. Since YAG inclusions limit alumina grain growth composites show essentially better wear resistance than pure alumina and better than the 3YTZP materials.

Acknowledgment

Research was financially supported by the Polish Ministry of Science and High Education under grant NN 507 457737.

References

1. Claussen N. Fracture toughness of Al_2O_3 with an unstabilized ZrO_2 dispersed phase. *J Am Ceram Soc* 1976;**59**:49–51.
2. Matson LE, Hecht N. Microstructural stability and mechanical properties of directionally solidified alumina/YAG eutectic monofilaments. *J Eur Ceram Soc* 1999;**19**:2487–501.
3. Yoshida H, Nakamura A, Sakuma T, Nakagawa N, Waku Y. Anisotropy in high temperature deformation in unidirectionally solidified eutectic Al_2O_3–YAG single crystals. *Scr Mater* 2001;**45**:957–63.
4. Isobe T, Omori M, Uchida S, Sato T, Hirai T. Consolidation of Al_2O_3–$Y_3Al_5O_{12}$ (YAG) eutectic powder prepared from induction-melted solid and strength at high temperature. *J Eur Ceram Soc* 2002;**22**:2621–5.
5. Waku Y, Sakuma T. Dislocation mechanism of deformation and strength of Al_2O_3–YAG single crystal composites at high temperatures above 1500 °C. *J Eur Ceram Soc* 2000;**20**:1453–8.
6. Mah T, Parthasarathy TA, Matson LE. Processing and mechanical properties of Al_2O_3/$Y_3Al_5O_{12}$ (YAG) eutectic composites. *Ceram Eng Sci Proc* 1990;**11**:1617.
7. Ochiai T, Ueda T, Sato K, Hojo M, Waku Y, Nakagawa N, et al. Deformation and fracture behaviour of an Al_2O_3/YAG composite from room temperature to 2023 K. *Compos Sci Technol* 2001;**61**:2117–28.
8. Harada Y, Suzuki T, Hirano K, Waku Y. Ultra-high temperature compressive creep behaviour of an in-situ Al_2O_3 single crystal/YAG eutectic composite. *J Eur Ceram Soc* 2004;**24**:2215–22.
9. Ramirez-Rico J, Pinto-Gómez AR, Martinez-Fernandez J, de Arellano-López AR, Oliete PB, Pena JI, et al. High temperature plastic behaviour of Al_2O_3–$Y_3Al_5O_{12}$ directionally solidified eutectics. *Acta Mater* 2006;**54**:3107–16.
10. Wang S, Akutsu T, Tanabe Y, Yasuda E. Phase composition and microstructural characteristics of solidified Al_2O_3-rich spinel solid solution/YAG composite. *J Eur Ceram Soc* 2000;**20**:39–43.
11. Li WQ, Gao L. Processing, microstructure and mechanical properties of 25 vol% YAG–Al_2O_3 nanocomposites. *Nanostruct Mater* 1999;**11**:1073–80.
12. Wang H, Gao L. Preparation and microstructure of polycrystalline Al_2O_3–YAG composites. *Ceram Int* 2001;**27**:721–3.
13. Palmero P, Simone A, Esnout C, Fantozzi G, Montanaro L. Comparison among different sintering routes for preparing alumina–YAG nanocomposites. *J Eur Ceram Soc* 2006;**26**:941–7.
14. Okada K, Motohashi T, Kameshima Y, Yasumori A. Sol–gel synthesis of YAG/Al_2O_3 long fibres from water solvent systems. *J Eur Ceram Soc* 2000;**20**:561–7.
15. Towata HJ, Hwang M, Yasuoka M, Sando K, Niihara. Preparation of polycrystalline YAG/alumina composite fibres YAG fibres by sol–gel method. *Composites Part A* 2001;**32**:1127–31.
16. Gao L, Shen A, Miyamoto H, Nygren M. Superfast densification of oxide/oxide ceramic composites. *J Am Ceram Soc* 1999;**82**:1061–3.
17. Palmero P, Naglieri V, Chevalier J, Fantozzi G, Montanaro L. Alumina based nanocomposites obtained by dopping with inorganic salt solutions: application to immiscible and reactive systems. *J Eur Ceram Soc* 2009;**29**:59–66.

18. Palmero P, Lomello F, Fantozzi G, Bonnefont G. Alumina–YAG micro-nanocomposites: elaboration and mechanical characterization. In: *Proceedings of the 11th International Conference of the European Ceramic Society, Krakow, June 2009, session: F*. 2009. p. 669–76.
19. Schehl M, Diaz LA, Torrecillas R. Alumina nanocomposites from powder–alkoxide mixtures. *Acta Mater* 2002;**50**:1125–39.
20. Torrecillas R, Schehl M, Diaz LA, Menendez LJ, Moya JS. Creep behaviour of alumina/YAG nanocomposites obtained by a colloidal processing route. *J Eur Ceram Soc* 2007;**27**:143–50.
21. Gao L, Shen A, Miyamoto H, Nygren M. Superfast densification of oxide/oxide ceramic composites. *J Am Ceram Soc* 1999;**82**: 1061–110.
22. Palmero P, Naglieri V, Spina G, Montanaro L. Elaboration and mechanical characterization of Al_2O_3–ZrO_2–YAG ultrafine composites. *Poster presented at CIMTEC conference*, Montecatini Terme, June 2010.
23. Lach R, Haberko K, Trybalska B. Composite material in the Al_2O_3–20 vol.% YAG system. *Proc Appl Ceram* 2010;**4**:1–6.
24. Lach R, Haberko K. Particulate composites in the Al_2O_3–YAG system. In: *Proceedings of the 11th ECerS conference, Krakow, June 2009*. 2009.
25. Niihara K, Morena R, Hasselman PPH. Evaluation of K_{Ic} brittle solids by the indentation method with low crack-to-indent ratios. *J Mater Sci Lett* 1981;**2**:13–6.
26. Niihara K. A fracture mechanics analysis of indentation indentation-induced Palmqvist crack in ceramics. *J Mater Sci Lett* 1983;**2**:221–3.
27. Barsoum MW. *Fundamentals of ceramics*. International Editions: McGraw-Hill; 1997 [chapter 11].
28. Piekarczyk J, Hennicke HW, Pampuch R. On determining elastic constants of porous zinc ferrite materials. *cfi/BerDKG* 1982;**59**:227–32.
29. Glasner A, Levy E, Steinberg M. Thermal decomposition of yttrium oxalate in vacuum and in various atmospheres. *J Inorg Nucl Chem* 1963;**25**:1119–27.
30. Haberko K. Characteristics and sintering behaviour of zirconia ultrafine powders. *Ceram Int* 1979;**5**(4):145–8.
31. Kellet BJ, Lange FF. Thermodynamics of densification: I, simple particle arrays, equilibrium configuration, pore stability and shrinkage. *J Am Ceram Soc* 1989;**72**:725–34.
32. Lange FF, Kellet BJ. Thermodynamics densification: II grain growth in porous compacts and relation to densification. *J Am Ceram Soc* 1989;**72**:735–41.
33. Kuczynski GC. Sintering in multicomponent systems. In: Kuczynski GC, Hooton NA, Gibbon CF, editors. *Sintering and related phenomena*. New York, London, Paris: Gordon and Breach, Science Publishers; 1967, p 685.
34. De Jonghe LC, Rahaman MN. Sintering of ceramics. In: Somiya S, et al., editors. *Handbook of advanced ceramics*. Amsterdam, Boston, Heidelberg, London, New York, Oxford, Paris, San Diego, San Francisco, Singapore, Sidney, Tokyo: Elsevier Academic Press; 2003 [chapter 4].
35. Scherer GW. Sintering with rigid inclusions. *J Am Ceram Soc* 1987;**70**:719–25.
36. Faber KT, Evans AG. Crack deflection process, part I and II. *Acta Metall* 1983;**31**:565–84.
37. Rice RW. Ceramic matrix composites: an update. *Ceram Eng Sci Proc* 1985;**6**:589–607.